2004

Synthesis and Structure of Five Sc3CuyZn18-y-Type Compositions (0 ≤ y ≤ ~2.2), 1/1 Crystalline Approximants of a New Icosahedral Quasicrystal. Direct Example of Tuning on the Basis of Size Effects and Hume–Rothery Concepts

Qisheng Lin
The Ames Laboratory, qslin@ameslab.gov

John D. Corbett
Iowa State University

Inorg. Chem. **2004**, *43*, 1912–1919

Synthesis and Structure of Five $Sc_3Cu_yZn_{18-y}$-Type Compositions ($0 \leq y \leq \sim 2.2$), 1/1 Crystalline Approximants of a New Icosahedral Quasicrystal. Direct Example of Tuning on the Basis of Size Effects and Hume–Rothery Concepts

Qisheng Lin and John D. Corbett*

Department of Chemistry, Iowa State University, Ames, Iowa 50011

Received August 29, 2003

The newly reported icosahedral quasicrystalline phase $\sim Sc_3Cu_{2.1}Zn_{12.9}$ was approached through four synthetic, structural, and EDX analyses of the range of approximants formed by systematic substitutions of 0–4 Zn by Cu in the reported Sc_3Zn_{17} as well as for the corrected Sc_3Zn_{18} ($ScZn_6$) composition. Structures of high yield products of the 0, 1, 2, 3 Cu atom steps all refined as isotypic $Sc_3Cu_yZn_{18-y}$ phases ($Im\bar{3}$, $Z = 8$, $a = 13.8311(5)$ to $13.7528(5)$ Å for $0 \leq y \leq 2.2$), basically isostructural with RCd_6 phases known for many rare-earth elements. The present phases all exhibit the novel feature of disordered zinc tetrahedra in the center of four concentric polyhedral clusters: pentagonal dodecahedron (Zn/Cu), icosahedron (Sc), icosidodecahedron (Zn), and triacontahedron (Zn). The Cu tuning process reduces both the average electron count per atom (e/a) to 2.04 and the average atom size until major amounts of the zinc-poorer quasicrystal separate along with the present normal crystalline phase near four added Cu. The Cu is an important neighbor to the disordered Zn atoms. The approximant structure repeatedly exhibits components with pseudo-icosahedral symmetry.

Introduction

Quasicrystal (QC) phases are a novel class of intermetallic compounds with rotational symmetries in their diffraction patterns that are incommensurate with translational periodicity.[1] They are generally regarded as electron phases, as described for example by Hume−Rothery rules,[2] and probably have band gaps or pseudogaps at or near the Fermi energy.[3] In addition, atomic size factors have been reported to play a critical role in quasicrystal formation.[4] The optimized valence electron count per atom (e/a) for icosahedral quasicrystals was first considered to be in the range of 2.1−2.2,[5] but this was reduced to 2.0 with advent of the remarkable binary QC examples $CaCd_{5.75}$ and $YbCd_{5.75}$.[4,6] The known quasicrystals plus their presumed approximants are extensively utilized to generalize experience in the study of quasicrystals. The approximants are translationally normal crystalline compounds with customarily large unit cells that contain condensed high-symmetry building blocks such as icosahedra and dodecahedra and have compositions close to those of the related quasicrystals.

The approximants to the above quasicrystals were originally taken to be $YbCd_6$[7] and $CaCd_6$[8] although the recently discovered $CaCd_{5.85}$[9] may be even more appropriate. According to what we conclude here was the first generally correct structure for the former pair, that reported by Larson and Cromer[10] for YCd_6, these assumed approximants evidently exhibit a common motif of a body-centered cubic ($Im\bar{3}$) lattice containing a symmetry-breaking disordered tetrahedron around the origin that is surrounded concentrically by multiply endohedral ordered clusters, a pentagonal

* Author to whom correspondence should be addressed. Phone: 515-294-3086. Fax: 515-294-5718. E-mail: jcorbett@iastate.edu.

(1) Shechtman, D.; Blech, I.; Gratias, D.; Cahn, J. W. *Phys. Rev. Lett.* **1984**, *53*, 1951. Goldman, A. I.; Kelton, R. F. *Rev. Mod. Phys.* **1993**, *65*, 213. Janot C. *Quasicrystals: A Primer*, 2nd ed.; Oxford University Press: Oxford, U.K., 1994.
(2) Hume−Rothery, W. *J. Inst. Metals* **1926**, *35*, 295.
(3) Tsai, A. P. In *Physical Properties of Quasicrystals*, Stadnik, Z. M., Ed.; Springer: New York, 1999; p 5. Takeuchi, T.; Sato, H.; Mizutani, U. *J. Alloys Compd.* **2002**, *342*, 355.
(4) Tsai, A. P.; Guo, J. Q.; Abe, E.; Takakura, H.; Sato, T. J. *Nature* **2000**, *408*, 537.
(5) Tsai, A. P. In *Physical Properties of Quasicrystals*; Stadnik, Z. M., Ed.; Springer: New York, 1999; p 23.
(6) Guo, J. Q.; Abe, E.; Tsai, A. P. *Phys. Rev. B.* **2000**, *62*, R14605.
(7) Palenzona, A. *J. Less-Common Met.* **1971**, *25*, 367.
(8) Bruzzone, G. *Gazz. Chim. Ital.* **1972**, *102*, 234.
(9) Gomez, C. P.; Lidin, S. *Angew. Chem., Int. Ed.* **2001**, *40*, 4037.
(10) Larson, A. C.; Cromer, D. T. *Acta Crystallogr.* **1971**, *27B*, 1875.

10.1021/ic030265p CCC: $27.50
Published on Web 02/19/2004

Table 1. Loaded Compositions, Guinier Cell Parameters ($Im\bar{3}$), and EDX and X-ray Refinement Results for Approximant Phase Samples[a]

loaded compositions		products			
			EDX composition		X-ray refined composition
x	$Sc_3Cu_xZn_{17-x}$	latt. const.[a] (Å)	at. % (Sc/Cu/Zn)	empirical	$\sim Sc_3Cu_yZn_{18-y}$
0	Sc_3Zn_{17}	13.8311(5)	15.3(2)/84.7(9)	$Sc_3Zn_{16.64}$	$Sc_3Zn_{18.0}$
1	$Sc_3Cu_{1.0}Zn_{16.0}$	13.7923(5)	14.5(2)/3.1(3)/82.4(9)	$Sc_3Cu_{0.64}Zn_{17.0}$	$Sc_3Cu_{0.65}Zn_{17.4}$
2	$Sc_3Cu_{2.0}Zn_{15.0}$	13.7598(6)	14.5(2)/7.0(3)/78.5(9)	$Sc_3Cu_{1.45}Zn_{16.24}$	$Sc_3Cu_{1.48}Zn_{16.5}$
3	$Sc_3Cu_{3.0}Zn_{14.0}$	13.7528(5)	14.6(2)/10.4(3)/75.0(9)	$Sc_3Cu_{2.14}Zn_{15.4}$	$Sc_3Cu_{2.19}Zn_{16.0}$
4	$Sc_3Cu_{4.0}Zn_{13.0}$	[13.7469(5)][b]	15.4(2)/13.5(3)/71.1(9)	$Sc_3Cu_{2.63}Zn_{13.85}$	

[a] Equilibrated at 200 °C. [b] Uncertain because of ~70% admixed quasicrystal phase. Other products were ~single phase.

dodecahedron, an icosahedron, an icosidodecahedron, and so on. The RCd_6 (and $CaCd_6$) structures for a wide variety of rare-earth metals R (and Ca) have been recently put on a much firmer basis by the thorough crystallographic studies of Gómez and Liden.[11] They in fact observed an amazing array of different configurations for the central disordered atoms in Fourier maps, ranging from tetrahedra to almost continuous "cubes", as well as some moderately small off-stoichiometries in certain compounds.

In contrast, the discoverers of the Mg−Sc−Zn quasicrystal[12] concluded that its approximant was Sc_3Zn_{17},[13] evidently not noting the doubts raised about this structure and composition by the study of YCd_6. The cubic structure type reported for Sc_3Zn_{17} is exactly that of YCd_6 etc. *except* that the innermost disordered atoms are not present, leaving a huge hole instead. Thus, Larson and Cromer in their careful study of the isotypic YCd_6[10] ($\cong Y_3Cd_{18}$) wondered whether this feature also belonged in Sc_3Zn_{17} (and in the reported isotypic phases Ru_3Be_{17}, etc.[14,15] as well). The related Yb_3Zn_{17} has also been so assigned.[16]

Our investigations of the Sc−Cu−Zn system, following on the above information, have taken two directions. First, starting with the reported Sc_3Zn_{17}, explorations of $Sc_3Cu_xZn_{17-x}$ compositions for $x = 0-4$, chosen so as to reduce e/a from 2.15 by substitution of Cu for Zn, led us into the present work, the discovery of a presumed approximant phase region $Sc_3Cu_yZn_{18-y}$ with range of compositions at 200 °C of about $0 \leq y \leq 2.2$. We will show that different compositions therein are all based on evident copper substitution for zinc in the YCd_6 (RCd_6) type structure of $ScZn_6$ and all include the centered disordered Zn_4 tetrahedron. Thus, the first member of the series Sc_3Zn_{18}, or $ScZn_6$, replaces Sc_3Zn_{17}. The study provides a good example of tuning on the basis of size and electronic rules. Before this came our more empirical discovery of a new quasicrystalline phase with a slightly different composition, $\sim Sc_{16.5}Cu_{11.7}Zn_{71.7}$ ($\cong Sc_3Cu_{2.1}Zn_{12.9}$), $e/a = 2.04$, that separates at 480 °C.[17]

Experimental Section

Syntheses. Starting elements of Sc chunks (99.9%, APL-Aldrich), Cu powder (99.9%, Alfa) and Zn shot (99.9%, Alfa) were used as received. Following the reported composition Sc_3Zn_{17}, five alloys with target compositions $Sc_3Cu_xZn_{(17-x)}$ for $x = 0, 1, 2, 3, 4$ (e/a values of 2.15, 2.1, 2.05, 2.00, 1.95) were synthesized to approach the new quasicrystal. This step took place through melting the weighed elements together in a Ta container that had been weld-sealed within an argon atmosphere. The container itself had been further enclosed within an evacuated SiO_2 jacket to avoid its air oxidation. The samples were melted at 700 °C for 2 h to homogenize them, cooled to 570 °C within 10 min, and then slowly cooled to 420 °C at a rate of 5 °C /h for crystal growth. Finally, the samples were annealed at 200 °C for several days to gain equilibrium and better quality crystals.

The products, which have a metallic luster and are a little brittle, were first examined under a microscope inside a glovebox filled with purified nitrogen. Candidate crystals were selected from small crushed pieces and inserted in thin-walled glass capillaries for preliminary checks with the aid of Laue photographs, and the remainders of the samples were ground for powder X-ray diffraction to check the phase purity and to refine the cell parameters. Some crystals were also exposed to room-temperature air for over one week to see whether they were stable. No color or surface changes were observed under the microscope, and no weight change was measured. Therefore, later processes with the products were carried out in the air.

Analyses. To better define the end compositions of the compounds obtained, semiquantitative energy-dispersive X-ray spectroscopy (EDX) and inductively coupled plasma (ICP) techniques were utilized. The former analyzed cleaved, apparently flat, and clean surfaces of crushed bulk crystals on a JEOL 840A SEM/IXRF instrument, whereas 0.1−0.2-mm bulk crystals were visually selected under low magnification for ICP analyses.

Powder X-ray Diffraction. X-ray powder diffraction data were secured with the aid of a Huber 670 Guinier powder camera equipped with an area detector and Cu $K\alpha_1$ radiation ($\lambda = 1.540\,598$ Å). Powdered samples were homogeneously dispersed on a flat Mylar surface with the aid of a little petrolatum. The step size was set at 0.005° and the exposure time was 1 h. Data acquisition was controlled via the in-situ program. Peak search, indexing, and least-squares refinements for cell parameters were done with the aid of Winplotr and its built-in programs.[18] The results showed that the main products were substantially single-phase (>95−97%) cubic crystalline approximants for $x \leq 3$, whereas a mixture of about 30% approximant and ~70% quasicrystal phase was found in the $x = 4$ product. Table 1 lists the refined cell parameters

(11) Gómez, C. P.; Lidin, S. *Phys. Rev. B.* **2003**, *68*, 024203.
(12) Kaneko, Y.; Arichika, Y.; Ishimasa, T. *Philos. Mag. Lett.* **2001**, *81*, 777.
(13) Andrusyak, R. I.; Kotur, B. Ya.; Zavodnik, V. E. *Sov. Phys. Crystallogr.* **1989**, *34*, 600.
(14) Sands, D. E.; Johnson, Q. C.; Kikorian, O. H.; Kromholtz, K. L. *Acta Crystallogr.* **1962**, *15*, 1191.
(15) Villars, P.; Calvert, L. D. *Pearson's Handbook of Crystallographic Data for Intermetallic Phases*, 2nd ed; American Society of Metals: Materials Park, OH, 1991; Vol. 1, p 169, 2195.
(16) Bruzzone, G.; Fornasini, M. L.; Merlo, F. *J. Less-Common. Met.* **1970**, *22*, 253.
(17) Lin, Q. S.; Corbett, J. D. *Philos. Mag. Lett.* **2003**, *83*, 755.
(18) Roisnel, T.; Rodriguez-Carvajal, J. In *Materials Science Forum, Proceedings of the Seventh European Powder Diffraction Conference (EPFIC 7)*; Delhez, R., Mittenmeijer, E. J., Eds.; 2000, p 118.

obtained, which were used later in bond distance calculations, the EDX analyses, and the compositions of the crystals refined for the first four. The ICP analyses (not given) had better accuracies, but the stoichiometries thereby determined for $x = 1, 2, 3$ largely only confirmed the compositions loaded, indicating the simple crystal picking had not been successful. In contrast, the EDX results were uniformly 30−32% lower in copper content than loaded and clearly more consistent with the X-ray structural refinements, thereby reflecting fractionation of a small amount of copper into an unseen minor phase.

Crystallography. Good-quality single crystals were mounted on a Siemens APEX Platform CCD diffractometer equipped with graphite-monochromatized Mo Kα radiation, and diffraction data were collected at ∼293 K over a hemisphere of reciprocal space up to $2\theta = 56.46°$. The individual frames were measured with an ω rotation of 0.3° and an acquisition time of 15 s. The SMART software was used for the data acquisition, SAINT was used for the data extraction and reduction, and SADABS was used for absorption correction; all were in the program package. Structure solutions and refinements were performed using the SHELXTL package of crystallographic programs.[19] All data sets showed the systematic absence condition (*hkl*: $h + k + l = 2n$, etc.), allowing three possible space groups, $I23$, $I2_13$ and $Im\bar{3}$. However, the E-Stats model as implemented in the WinGX program[20] strongly suggested that each structure was centrosymmetric, so the space group was tentatively taken to be $Im\bar{3}$. All structures were successfully solved therein by direct methods. Seven atoms were first located, and the first six were initially assigned to Zn atoms and the last one was assigned to Sc on the basis of the peak heights and bond distances.

For the binary product ($x = 0$), subsequent isotropic least-squares refinements proceeded smoothly to R1 = 12.1%, wR2 = 30.9%, GOF = 1.09, at which point the largest difference electron densities were +11.0 and −10.8 $e^-Å^{-3}$. However, three zinc atom sets on the 12*d* (Zn4), 16*f* (Zn5), and one of the 24*g* (Zn6) positions had somewhat larger displacement parameters ($10^3\ U_{eq} = 17 - 24$) than did the other four, which suggested that the three might have partial occupancies. Accordingly, both the occupancy and isotropic parameters for each of the three Zn atoms were successively allowed to refine with the others held at full occupancy. The results indicated full occupancy for each within 2σ, that is, between 98(2)% and 104(3)%. The larger displacement parameters of the three Zn atoms therefore must result for structural reasons.

At this stage, the largest electron density in the ΔF map appeared to be a false peak only 0.53 Å from Zn5, but the second one on a 24*g* position (10.8 $e^-Å^{-3}$) was a feasible addition because it was ∼2.22 Å from its nearest neighbor (Zn5). An additional Zn7 atom at this point then refined to a variable occupancy of 0.300(5). This position generates what has been described as a 3-fold disordered tetrahedron in YCd_6 by Larson and Cromer,[10] so the occupancy was fixed at 1/3. The final anisotropic least-squares refinements, with 47 parameters and 608 independent reflections with $I > 2\sigma(I)$ converged at R1 = 2.77%, wR2 = 6.12% and GOF = 1.09. Residual electronic densities then ranged between 5.92 $^-Å^3$, 1.52 Å from Zn7, and −1.59 $e^-Å^{-3}$, 1.14 Å from Zn7.

The last two features actually both reflect the apparent unusual distribution of the Zn7 atoms (below). Their large isotropic parameters U (∼$99(3) \times 10^{-3}$) or extreme anisotropic displacement values (∼4:1 for the principal axes with relatively small σ's) are again characteristic of the disordered tetrahedron of Zn7. The elongated and diffuse nature of these densities are clear in a Fourier map of the region (below). A 3-fold disorder of a tetrahedron seems more reasonable than an assignment as a single rather distorted icosahedron at one-third occupancy. The general similarity to the YCd_6[10] (and RCd_6) results is striking.

Table 2. Some Crystallographic Collection and Refinement Data

refined composition	$(ScZn_6)_3$	$Sc_3Cu_{1.48}Zn_{16.5}$
f.w.	1311.9	1307.9
space group, *Z*	$Im\bar{3}$, 8	$Im\bar{3}$, 8
latt. param:[a] *a* (Å)	13.8311(5)	13.7598(6)
V ($Å^3$)	2645.9(2)	2605.2(2)
dcalc (g/cm^3)	6.554	6.674
μ (Mo Kα (mm^{-1})	33.14	33.52
R1, wR2 (%)[b]	2.77, 6.02	2.87, 5.52

[a] Huber diffractometer data, $\lambda = 1.540598$ Å, 23 °C. [b] $R1 = \Sigma||F_o| - |F_c||/\Sigma|F_o|$; $wR2 = [\Sigma w(|F_o|^2 - |F_c|^2)^2/\Sigma w(F_o^2)]^{1/2}$.

Very similar results were obtained for crystals from reactions loaded for $x = 1$, 2, and 3, including the generic characteristics of the displacement parameters and invariant occupancies of the Zn4, Zn5, and Zn6 sites (Table 2 and Supporting Information). Considering that mixing of Cu and Zn on the same sites is common in many other compounds (e.g., Cu_3Zn,[21] $Ca_5Cu_3Zn_2$,[22] and Al_4Cu_3Zn[23]), it was presumed a similar event might occur in the three ternaries analyzed. But variations of such proportions along with a single isotropic displacement parameter for each of the three normal (smaller) Zn positions as well gave only negative Cu occupancies. Possibilities of mixing Cu on most other Zn positions was also excluded because these resulted in either negative occupancies, unstable refinements, or extremely large standard deviations. On the other hand, the chemical analyses and variations among both the cell parameters and the atom positions with respect to composition (Tables 1 and 2, Supporting Information) made clear that Cu and Zn do form some sort of solid solution in a slowly changing structure in this region, as difficult as it may be to distinguish low copper contents (∼4−12% overall) because of the very similar X-ray scattering by Cu and Zn. The displacement parameters were usually largest for Zn5, and this atom also showed three distinctive features: (1) ∼0.25 Å shorter separations from the fractional Zn7 (2.26 Å) (which may not be too unusual), (2) Zn5−Zn5 distances that are about 0.13 Å shorter than those for other like bonds in the normal pentagonal dodecahedron that surrounds the origin (≤2.53 Å vs 2.66 Å), and (3) two of the few decreases in distances on Cu substitution, in the longer Zn5−Zn5 and Sc−Zn5 distances (Table 4 and Table S4 in the Supporting Information). Therefore, an amount of Cu in only the Zn5 position was fixed according to its proportion in the EDX results in the three pseudo-ternary structural refinements of nominal $x = 1$, 2, and 3 products. The results of these studies thus refined to compositions $Sc_3Cu_yZn_{18-y}$ for $y = 0$, 0.65, and 1.49. An additional small amount of Zn, ∼24(2)%, in a new fixed 8*c* position was found in the fourth $x = 4$ product, making its refined composition $Sc_3Cu_{2.19}Zn_{16.0}$ ($y = 2.19$). This is the only significant example of nonstoichiometry and parallels those observed in some RCd_6 studies.[11]

Table 2 lists some crystallographic data, and Table 3 contains the corresponding atomic positions and isotropic-equivalent displacement parameters for the Sc_3Cd_{18} and $Sc_3Cu_{1.48}Zn_{16.5}$ products ($x = 0$, 2). Distances in these two are listed in Table 4. Positional and distance data for the other two structures ($y = 0.65$, 2.19),

(19) SHELXTL.; Bruker AXS, Inc.; Madison, WI, 1997.
(20) Farrugia, L. J. *J. Appl. Cryst*. **1999**, *32*, 837.
(21) Ng, S. C.; Brockhouse, B. N.; Hallman, E. D. *Mater. Res. Bull*. **1967**, *2*, 69.
(22) Merlo, F.; Fornasini, M. L. *J. Less-Common Met.* **1985**, *109*, 135.
(23) Murphy, S. *Met. Sci*. **1975**, *9*, 163.

Table 3. Positional ($\times 10^4$) and Displacement Parameters ($\times 10^3$) for Sc_3Zn_{18} and $Sc_3Cu_{1.5}Zn_{16.5}$ ($x = 0, 2$)[a]

atom	Wyckoff	site symm.	*x*	*y*	*z*	*U*(eq)[b]	occupancy:Zn/Cu[c]
Zn1	12*e*	mm2..	1901(1)	0		9(1)	
			1895(1)	0		8(1)	
Zn2	24*g*	m..	0	4044(1)	3457(1)	8(1)	
			0	4045(1)	3449(1)	6(1)	
Zn3	48*h*	1	1169(1)	3407(1)	1998(1)	12(1)	
			1144(1)	3426(1)	2001(1)	8(1)	
Zn4	12*d*	mm2..	4053(1)	0	0	20(1)	
			4079(1)	0	0	15(1)	
Zn5/Cu	24*g*	m..	0	2382(1)	916(1)	24(1)	100/0
			0	2388(1)	912(1)	21(1)	78/22
Zn6	16*f*	.3.	1617(1)	1617(1)	1617(1)	17(1)	
			1626(1)	1626(1)	1626(1)	16(1)	
Zn7	24*g*	m..	0	748(6)	810(5)	99(3)	1/3Zn
			0	760(5)	823(5)	88(3)	1/3Zn
Sc	24*g*	m..	0	1898(1)	2997(1)	5(1)	
			0	1874(1)	3001(1)	4(1)	

[a] Parameters are listed in sequence for Sc_3Zn_{18} and $Sc_3Cu_{1.5}Zn_{16.5}$ phases. [b] *U*(eq) is defined as one-third of the trace of the orthogonalized U_{ij} tensor. [c] Mixed occupancy for Zn5/Cu was fixed at EDX proportion for the ternary crystal, while occupancy at Zn7 position was fixed at 1/3. The refined occupancies of Zn7 were 30.0(5)% and 33.3(6)%, respectively.

Table 4. Bond Distances (Å) in Two $Sc_3Cu_yZn_{18-y}$ Phases

bonds			Sc_3Zn_{18}	$Sc_3Cu_{1.48}Zn_{16.5}$	bonds			Sc_3Zn_{12}	$Sc_3Cu_{1.48}Zn_{16.5}$
Zn1	Zn2	2*x*	2.502(1)	2.496(1)	Zn5	Zn7	1*x*	2.264(8)	2.166(6)
	Zn2	2*x*	2.526(1)	2.510(1)		Zn5	1*x*	2.534(2)	2.510(2)
	Zn3	4*x*	2.7360(6)	2.6824(7)		Zn3	2*x*	2.620(1)	2.600(1)
	Zn4	2*x*	2.938(1)	2.899(1)		Zn4	1*x*	2.636(2)	2.644(2)
	Sc	2*x*	3.231(1)	3.229(2)		Zn6	2*x*	2.6572(8)	2.6592(9)
Zn2	Zn1	1*x*	2.502(1)	2.496(1)		Zn7	2*x*	2.720(8)	2.805(7)
	Zn1	1*x*	2.526(1)	2.510(1)		Sc	1*x*	2.955(2)	2.961(2)
	Zn2	1*x*	2.645(2)	2.628(2)		Sc	2*x*	3.037(1)	2.990(1)
	Zn3	2*x*	2.6824(8)	2.6608(8)	Zn6	Zn3	3*x*	2.6060(9)	2.6141(9)
	Zn3	2*x*	2.7321(9)	2.6789(9)		Zn5	3*x*	2.6572(8)	2.6592(9)
	Zn4	2*x*	2.832(1)	2.809(1)		Zn7	3*x*	2.774(3)	2.766(3)
	Sc	1*x*	3.035(2)	3.049(2)		Sc	3*x*	2.9656(9)	2.9507(9)
	Sc	2*x*	3.109(1)	3.080(1)	Sc	Zn3	2*x*	2.919(1)	2.9119(1)
Zn3	Zn6	1*x*	2.6060(9)	2.6141(9)		Zn5	1*x*	2.955(2)	2.961(2)
	Zn5	1*x*	2.620(1)	2.600(1)		Zn6	2*x*	2.9656(9)	2.9507(9)
	Zn3	2*x*	2.6621(9)	2.6853(9)		Zn3	2*x*	2.980(1)	2.988(1)
	Zn2	1*x*	2.6824(8)	2.6608(8)		Zn3	2*x*	2.9954(8)	2.9878(8)
	Zn2	1*x*	2.7321(9)	2.6789(9)		Zn4	1*x*	3.004(1)	2.975(2)
	Zn1	1*x*	2.7360(6)	2.6824(7)		Zn2	1*x*	3.035(2)	3.049(2)
	Sc	1*x*	2.919(1)	2.911(1)		Zn5	2*x*	3.037(1)	2.990(1)
	Sc	1*x*	2.980(1)	2.988(1)		Zn2	2*x*	3.109(1)	3.080(1)
	Sc	1*x*	2.9954(8)	2.9878(8)	Zn7	Zn5	1*x*	2.264(8)	2.260(1)
Zn4	Zn4	1*x*	2.621(3)	2.534(3)		Zn5	2*x*	2.720(8)	2.766(3)
	Zn5	2*x*	2.636(2)	2.644(2)		Zn6	2*x*	2.774(3)	2.805(7)
	Zn2	4*x*	2.832(1)	2.809(1)					
	Zn1	2*x*	2.938(1)	2.899(1)					
	Sc	2*x*	3.004(1)	2.975(2)					

general data collection and refinement parameters, and anisotropic displacement data for all studies are contained in the Supporting Information.

A synthesis reaction with the stoichiometry refined for the binary, $ScZn_6$ (Sc_3Zn_{18}) was later run under the same conditions. A crystal therefrom gave a 0.022 Å (20σ) larger cell parameter (13.853(1) Å) than for the $x = 0$ product (which solved as essentially Sc_3Zn_{18}). This fifth single crystal structure solution (residuals of 3.7, 6.3%) revealed the same structure motif with only small changes, mainly in the slightly greater occupancy of the disordered Zn7 atom, 35.0(8)% vs 30.0(5)% before, and some small positional shifts (see Supporting Information). The occupancies lead literally to crystallographic compositions $Sc_3Zn_{18.05(2)}$ vs $Sc_3Zn_{17.90(2)}$ before, a 5.3σ difference, suggesting a small nonstoichiometry *may* occur for the binary. The atom positional changes are principally for Zn5, by 17.6σ in *y*, and distances thereabout change by $4-7\ \sigma$, plus one at 15σ (Zn5−Zn6). The data are all contained in Table S5 in the Supporting Information.

Results and Discussion

In overview, these synthetic and crystallographic investigations of the Sc−Cu−Zn system over the stoichiometrics $Sc_3Cu_xZn_{17-x}$, $x = 0 - 4$, reveal the presence of a homogeneous phase region over much of this sample range. The lower limit is $ScZn_6$ (Sc_3Zn_{18}), a corrected composition and structure formerly reported as Sc_3Zn_{17}[11] that contains an additional disordered tetrahedron in an otherwise large hole around the origin, basically the same as that reported for YCd_6 30 years ago. (A related but erroneous structure for $YbZn_6$ has also been published.[24]) Otherwise, added Cu substitutes for Zn in substantially the same structure up to somewhat beyond $y = 2.2$. These features and the polyhedra that surround the tetrahedral distribution will be considered in detail later.

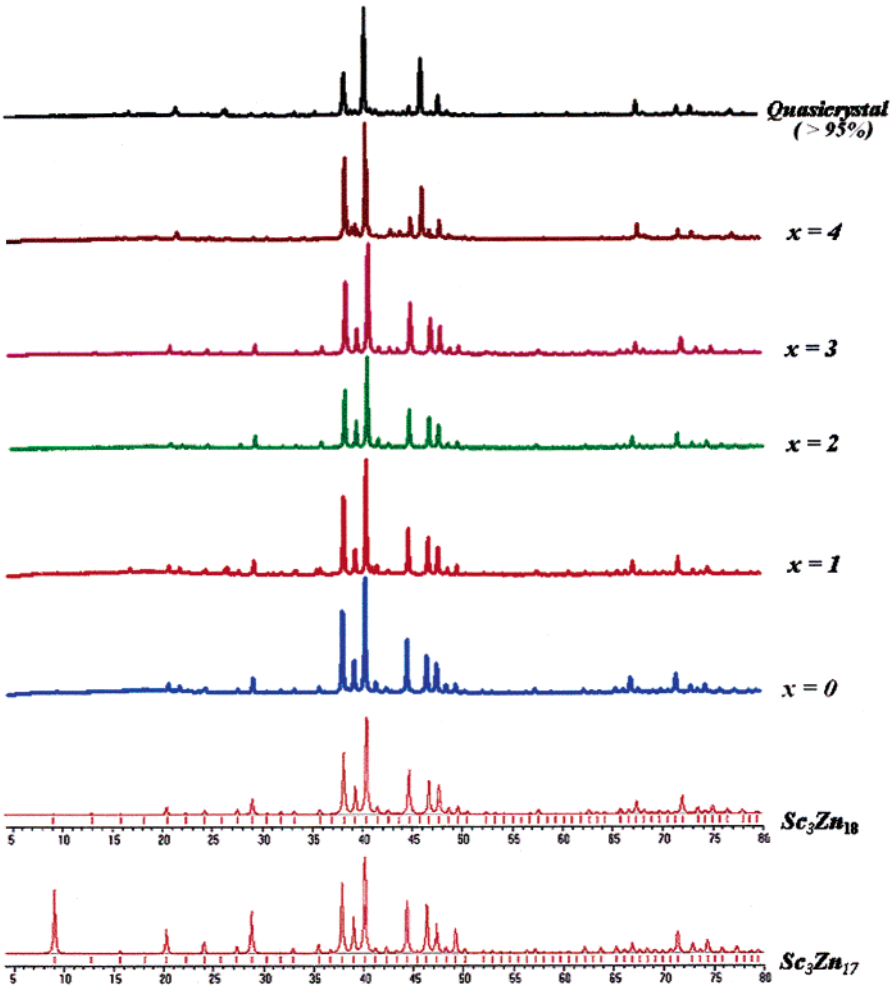

Figure 1. Observed Huber powder patterns (2θ) of nominal $Sc_3Cu_xZn_{17-x}$ synthesis products, $x = 0-4$. At the bottom are the powder patterns calculated from literature parameters for Sc_3Zn_{17} and our refined Sc_3Zn_{18} data ($x = 0$). At the top is the pattern of the quasicrystal $Sc_3Cu_{2.1}Zn_{12.9}$.[17]

At the other end of the region, the previously discovered and somewhat Zn-poorer quasicrystal phase $\sim Sc_3Cu_{2.1}Zn_{12.9}$ separates incongruently. This is the major component of a Cu-richer $x = 4$ product. (It should be noted that the approximant and quasicrystalline compositions are not quite comparable because the present samples were equilibrium products at 200 ° vs the 480 °C used in the QC isolation, and the copper content of the latter appears to decrease with decreasing temperature.)

The phase purities and the course of the changes across the entire phase region are evident in the Guinier powder data shown in Figure 1. This also demonstrates that the powder pattern calculated on the basis of the refined crystallographic positions for Sc_3Zn_{18} ($ScZn_6$) agrees very well with the experimental one ($x = 0$), whereas that at the bottom calculated from the atomic positions reported for Sc_3Zn_{17}[11] exhibits a large and anomalous intensity for the (110) reflection at ~9°. (This appears to have been missed in some subsequent literature assignments.) None of our experimental samples showed a stronger (110) reflection than expected from the Sc_3Zn_{18} result.

Other than for small positional shifts, the patterns for $x = 1$, 2, 3 agree very well with that for $ScZn_6$, whereas that for $x = 4$ clearly shows it to be a mixture with ~70% quasicrystalline phase (top pattern). Careful searching of the $x = 0-3$ patterns reveals three to four very weak and unassigned peaks in some (those at $2\theta = \sim 21.5°$ and ~23.8° are artifacts). Experimental patterns of the Sc_3Zn_{17} starting composition versus that for the Sc_3Zn_{18} product synthesized according to the refined composition show a clear but weak extra peak in the former near 38.3° and a possible second one at 39.3° in 2θ, which could come from the known Zn-poorer $Sc_{13}Zn_{58}$[25] (isostructural with $Gd_{13}Zn_{18}$[26]) (the strongest peak of $Sc_{13}Zn_{58}$ at ~40.1° overlaps that at ~40.12° for the phase studied). (A detailed comparison of these two patterns is given in the Supporting Information). The same may be true in the $x = 3$ and 4 products.

Structure Description. The basic structure can be described in several ways. Neglecting for the moment what is

(24) Palenzona[7] noted that the calculated density for the assigned composition and structure of Yb_3Cd_{17} was too low, so he added a full cadmium atom to an 8-fold site in the equivalent acentric group $I23$ to give the $YbCd_6$ stoichiometry, thus gaining a better agreement with (unreported) X-ray data. This result was transformed to the centric $Im\bar{3}$ when it was listed in *Pearson's Handbook*,[15] with the added Cd atom now at 50% in a 16*f* position, as opposed to the correct 33% in a 24*g* site (or equivalent) in RCd_6[11] and $ScZn_6$ (this work).

(25) Palenzona, A.; Manfrinetti, P. *J. Alloys Compd.* **1997**, *247*, 195.
(26) Wang, F. E. *Acta Crystallog.* **1967**, *22*, 579.

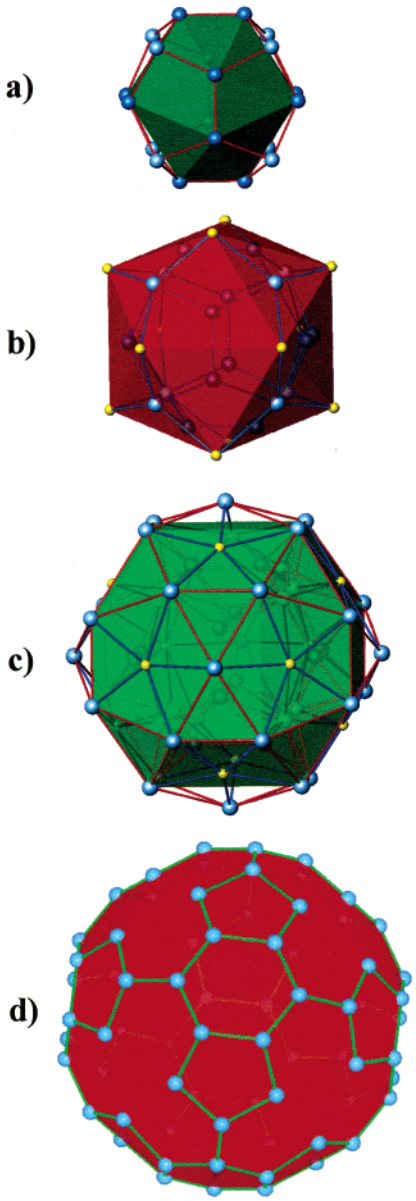

Figure 2. Successive ordered atom shells about the origin in $ScZn_6$ that surround the disordered Zn7 (not to scale): (a) dodecahedron of Zn5/Cu (darker blue) and Zn6; (b) icosahedron of Sc atoms (yellow) that cap the pentagonal face of the dodecahedron; (c) 30-atom shell of Zn3 and Zn4 atoms grouped along the cubic cell axes; and (d) the triacontahedral shell of Zn1, Zn2, and Zn3 atoms. Note that all surface atom pairs in (d) are not bonded. The isotypic structures containing Cu are generally very similar.

described as the 3-fold disordered $(Zn7)_4$ units around the origin, the regular part of the structure can be best described in terms of four successive concentric shells of atoms about that point. These total 138 atoms, terminating in a large 72-atom triacontahedron that is, in fact, condensed with other like members in the overall structure. Furthermore, the surface atoms on the last unit are not all interbonded, so it constitutes a more geometric formality.

The separate components of this multiply endohedral or concentric sphere model are shown in Figure 2. The first unit surrounding the disordered tetrahedra is a pentagonal-faced dodecahedron, Figure 2a, built of 12 Zn5/Cu atoms and eight Zn6 with radial distances from the origin of 3.53 and 3.87 Å, respectively. The distorted pentagonal faces are

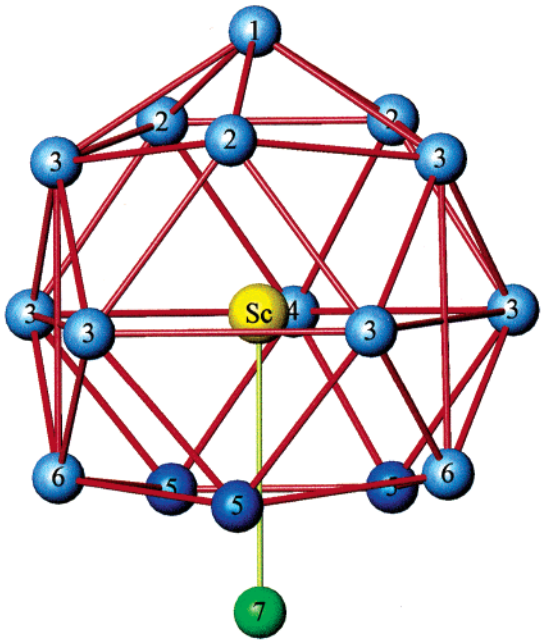

Figure 3. Environment of the Sc atom (yellow). Note the three pentagonal layers of Zn neighbors and the near Zn7 member (green) in the disordered tetrahedra. The last contact (3.47 Å) is marked.

all ordered (Zn6−Zn5−Zn5−Zn6−Zn5) and each Zn6 atom has three Zn5/Cu neighbors. The next collection of atoms are better described in two shells. In the first, Figure 2b, Sc atoms (yellow) cap the 12 pentagonal faces of the dodecahedron and thereby generate the dual isosahedron with a radius of 4.91 Å. The Zn6 cube also appears in these polyhedral faces as the slightly larger component of the inner dodecahedron. The next larger, Figure 2c, is a 30-atom Zn polyhedron (icosidodecahedron) built of what for the moment will be described as six flattened rectangular pyramids of Zn3 with Zn4 capping atoms on each that are ordered along the cubic axes (radius = 5.60−5.70 Å). Each Zn3 in this caps a Zn6−Zn5−Sc triangular face in 3b. Furthermore, the inner shell of Sc atoms is now seen to lie within Zn pentagons formed between these pyramids in which all Zn vertexes in each are members of two pentagons. The last polyhedron consists of a large zinc triacontahedron, Figure 2d, with radii of 7.0−7.4 Å in which normal Zn−Zn bond lengths do not appear on every edge. This is made of 12 Zn1, 36 Zn2, and 24 Zn3 atoms.

Alternatively, these four shells can also be usefully described in terms of the surroundings of each Sc atom in the above Sc icosahedron. The structure can thus be built from 12 condensed Sc-centered $Sc(Zn,Cu)_{16}$ polyhedra, one of which is shown in Figure 3. The Sc environment can be related to the components in Figure 2 in terms of the three condensed Zn pentagonal neighbors therein. These consist of the coplanar Zn3,4 rings (compare Figure 3c) that are bonded above to a distorted capped pentagon [Zn1-$(Zn2,Zn3)_5$] in the tricontahedron and below by the distorted pentagon of Zn5(Cu) and Zn6 that make up each dodecahedral face in Figure 3a. The Sc−Zn distances herein fall in a fairly narrow range of 2.92−3.11 Å. Finally, the topmost Zn1 atom in Figure 3 is somewhat more distant (3.23 Å), as

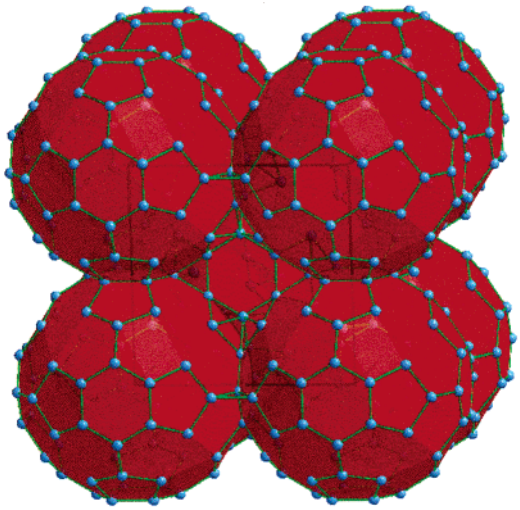

Figure 4. The bcc array of interpenetrating triacontahedra that describes the outer shell structure in $Sc_3Cu_yZn_{18-y}$, $0 \le y < 2.2$.

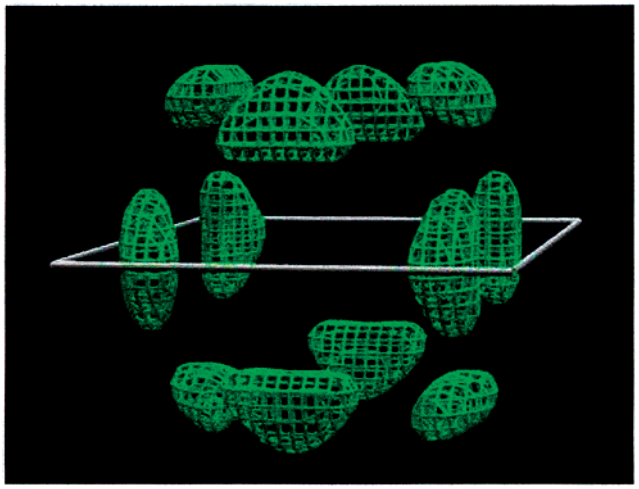

Figure 5. Perspective Fourier map of the disordered Zn7 atoms about the origin, which describe three disordered tetrahedra, each at 1/3 occupancy (contours at 6 $e^-/Å^3$). The refined positions lie at the centers of the 12 components.

is the nearest component of the external disordered Zn7 tetrahedra directly below (green, 3.47 Å) that will be described in the following section. (The next nearest Zn7 are 4.22 Å away.) The Sc atoms thus provide additional polar bonding within the Zn−Cu network and therewith some of the "glue" that holds the array of concentric clusters together. The polyhedron about Sc is related to, but not the same as, the Mackay[27] and Bergman[28] clusters often used in quasicrystal models. Finally, Figure 4 gives a general view of the bcc cell of $ScZn_6$ as built of shared, interpenetrating triacontrahedra, one of which was shown in Figure 3d. Shared hexagonal faces can be seen to propagate along the cell axes. The Zn1, Zn2, and Zn3 atoms on the surface of the tricontahedron described in Figure 3d are in fact all shared in the condensed result, Figure 4.

Disordered Tetrahedra. The five structures refined in the $Sc_3Cu_yZn_{18-y}$ series and from the direct Sc_3Zn_{18} synthesis exhibit a single very similarly disordered Zn7 site at close to one-third occupancy, the 12 centers of which describe a cubeoctahedron. In simple terms, this distribution can perhaps be best described in terms of three tetrahedra with their 3-fold axes appreciably displaced off the diagonal 3-fold axes of the unit cell. Even so, the position still refines with a large, anisotropic displacement parameter ($10^3\ U_{eq} \approx 90$). In distinct contrast to what the refinement can give in terms of centric ellipsoids, Figure 5 shows the Fourier map of the diffuse electron density in the region around the origin (symmetry $m\bar{3}$) in a perspective view, with contours drawn at 9 $e^-/Å^3$. This is closer to "the truth". There are still formally rather short Zn7−Zn7 distances of 2.24 Å within the tetrahedra between refined centroids, but the disorder, the larger standard deviations of the atomic positions, and, especially, the very anisotropic displacements deduced reflect appreciable positional disorder (and relaxation) within mean Zn7 positions, so probably no two Zn atoms have such a short separation.

A detailed description of the Zn7 disorder may be a good deal more complex, and we have used only the simplest explanation. Gómez and Lidin found a relatively wide selection of disorder characteristics for this position in their broad study of RCd_6 phases, a number of which are more complex than those seen here.[11] (They have also found ordered tetrahedra in an off-stoichiometry Eu_4Cd_{25}.[29]) It appears significant that the orientation of the highest density regions (centroids) among the disordered Zn7 atoms center on the Sc atoms and lie directly below the faces of the inner dodecahedron, Figure 3. (The angle Zn1−Sc−Zn7 is 177°.) This does not occur among the reported RCd_6 examples. Stronger Sc−Zn interactions might be expected between these smaller atoms.

The repeated icosahedral themes in this structure presumably are important in icosahedral quasicrystal formation as well as the *e*/*a* values and the change in average atom size with Cu substitution. It may also be significant that the quasicrystalline phase separates at about the point that the Zn5 atom (in our model) is completely replaced by Cu (see Supporting Information). Note that the decrease in lattice constant with *x* in Table 1 reflects the smaller size of Cu (0.037 Å less in single-bond metallic radii[30]), and that this also levels off at about the point of phase separation. The possible Cu saturation at this point may be significant in that three Zn5/Cu sites are the closest neighbors to the disordered Zn7, as seen at the bottom of Figure 3. Among the few distances that show clear decreases as the copper content increases are Zn(Cu)5−Zn(Cu5) (in the back in Figure 3 and across the top in Figure 2a) and two Sc−Zn-(Cu)5 contacts to the same atoms, which are among the larger of the 15 Sc−Zn values. Quasicrystal formation may indeed be accompanied by a distortion leading to a change in, or loss of, the Zn7 (dis)order. The principal macroscopic change on further condensation to form the QC is the elimination of Zn to give an empirical composition ~Sc_3-

(27) Mackay, A. L. *Acta Crystallogr.* **1962**, *15*, 916.
(28) Bergman, G.; Waugh, J. L. T.; Pauling, L. *Acta Crystallogr.* **1957**, *10*, 254.
(29) Gómez, C. P.; Lidin, S. *Chem., Eur. J.*, accepted.
(30) Pauling, L. *The Nature of the Chemical Bond*, 6th ed.; Cornell University Press: Ithaca, NY, 1960; p 403.

$Cu_{2.1}Zn_{12.9}$.[17] The quasicrystal with $e/a = \sim 2.04$ (at 480 °C) thus separates (~70%) from the $x = 4$ reaction (at 200 °C) along with a crystalline phase with the same e/*a* that contains more Cu and Zn according to the EDX data, Table 1.

The size proportions may be equally important, but further delineation of this feature in binary QC examples is limited to cadmium systems. The RCd_6 structure type occurs for nearly all rare-earth-metal−Cd systems; however, quasicrystal phases have been found only in the Ca−Cd and Yb−Cd systems. The metal single-bond radius ratios r_R/r_{Cd} may delineate the necessary size proportions fairly well in these systems, that is, between ratios for $CaCd_6$ (1.26[30]), $YbCd_6$ (1.23), and $EuCd_6$ (1.34), the last being the smallest R that is not known to form a QC. The lower limit may be reduced by present data; the weighted radius ratio for $Sc_3Cu_{2.1}Zn_{12.9}$ is a reasonable 1.16, although this now pertains to a Zn system. The tuning of Sc_3Zn_{17} to a quasicrystalline phase thus reduces *e*/*a* from 2.15 to ~2.04 as the size of the more "anionic" portion is suitably reduced by Cu substitution as well. The stability region of the normal phase at 200 °C may of course overlap some breadth in the QC composition at 480 °C. The recent discovery of the icosahedral quasicrystal $Sc_3Mg_{0.6}Cu_{9.6}Ga_{6.8}$[31] with $e/a = 2.01$ may be related. Presumably related QCs occur in $Sc_{15}M_{10}Zn_{75}$ systems, M = Ag, Au, Pd, Pt, but the compositions are not given.[32]

Finally, in another direction, the disordered Zn and Cd atoms found around the origins in $ScZn_6$ and RCd_6, respectively, could have been easily missed in the original structure reports for the isotypic parent Ru_3Be_{17} and so on because the disordered components would have been so very light. Otherwise, it's hard to imagine that a stable intermetallic structure would exist with such a large cavity, as noted before.[10]

Conclusion

In this paper, the crystal structures within the homogeneous approximant system $Sc_3Cu_yZn_{18-y}$ ($0 \le y < \sim 2.2$) were determined at four points to be the YCd_6-type ($Im\bar{3}$, $Z = 8$). The structure consists of a body-centered-cubic packing and condensation of 138-atom triacontahedra clusters, each of which contains three smaller concentric and interbonded cluster shells plus a disordered tetrahedron in the center. The homogeneous function within the approximant phase region consists mainly of the limited substitution of Zn in Sc_3Zn_{18} by Cu, a reasonable process in terms of size effects and Hume−Rothery electronic concepts.

Acknowledgment. We thank P. A. Thiel for her continued interest. This research was supported by the National Science Foundation, Solid State Chemistry, via grants DMR-9809850 and -0129785 and was performed in the Ames Laboratory, U.S. Department of Energy.

Supporting Information Available: Tables of crystal and refinement data, atomic positional, displacement ellipsoid, and distance summaries for three $Sc_3Cu_yZn_{18-y}$ products, together with similar data for the stoichiometric Sc_3Zn_{18}. A detailed comparison of impurity indications in the powder data for Sc_3Zn_{17} vs Sc_3Zn_{18}. This material is available free of charge via the Internet at http://pubs.acs.org.

IC030265P

(31) Kaneko, Y.; Maezawa, R.; Kaneko, H.; Ishimasa, T. *Philos. Mag. Lett.* **2002**, *82*, 483.
(32) Kashimoto, S.; Moezawa, Y.; Kasamo, Y.; Mitani, T.; Ishimasa, T. *Jpn. J. Appl. Phys. Lett.* **2003**, *42*, L1268.